Excitonic Magnetism in Van Vleck–type d^4 Mott Insulators

Giniyat Khaliullin

Max Planck Institute for Solid State Research, Heisenbergstrasse 1, D-70569 Stuttgart, Germany

(Received 31 July 2013; published 5 November 2013)

In Mott insulators with the t_{2g}^4 electronic configuration such as of Re^{3+}, Ru^{4+}, Os^{4+}, and Ir^{5+} ions, spin-orbit coupling dictates a Van Vleck–type nonmagnetic ground state with an angular momentum $J = 0$, and the magnetic response is governed by gapped singlet-triplet excitations. We derive the exchange interactions between these excitons and study their collective behavior on different lattices. In perovskites, a conventional Bose condensation of excitons into a magnetic state is found, while an unexpected one-dimensional behavior supporting spin-liquid states emerges in honeycomb lattices, due to the bond directional nature of exciton interactions in the case of 90° d-p-d bonding geometry.

DOI: 10.1103/PhysRevLett.111.197201 PACS numbers: 75.10.Jm, 75.25.Dk, 75.30.Et

Many transition metal (TM) compounds fall into a category of Mott insulators where strong correlations suppress low-energy charge dynamics, but there remains rich physics due to unquenched spin and orbital magnetic moments that operate at energies below the charge (Mott) gap. Depending on the spin-orbital structure of of constituent ions and the nature of the chemical bonding of neighboring d orbitals, the TM oxides host a great variety of magnetic phenomena [1] ranging from classical orderings to quantum spin and orbital liquids.

In broad terms, the magnetism of localized electrons in Mott insulators is governed by several factors: intraionic Hund's rules that form local spin S and orbital L moments; spin-orbit coupling (SOC) that tends to bind them into a total angular momentum $\boldsymbol{J} = \boldsymbol{S} + \boldsymbol{L}$; crystal fields which split d levels and suppress the L moment, acting thereby against SOC; and, finally, intersite superexchange (SE) interactions which establish a long-range coherence between spins and orbitals.

In Mott insulators with d orbitals of e_g symmetry, like manganites and cuprates, the L moment is fully quenched in the ground state (GS), and one is left with spin-only magnetism. In contrast, TM ions with threefold t_{2g} orbital degeneracy possess an effective orbital angular momentum $L = 1$, and a complex interplay between unquenched SOC and SE interactions emerges.

In TM oxides with an odd number of electrons on the d shell, S and J are half-integer; hence, the ionic GS is Kramers degenerate and magnetically active. The main effect of SOC in this case is to convert the original exchange interactions among S and L moments into an effective J Hamiltonian operating within the lowest Kramers J manifold. The t_{2g} orbital L interactions are bond dependent and highly frustrated [2]; consequently, the J Hamiltonians inherit this property, too. In short, SOC replaces $\boldsymbol{S}$ and $\boldsymbol{L}$ moments by $\boldsymbol{J}$ that obeys the same spin-commutation rules, but resulting magnetic states may obtain a nontrivial structure, as found for $d^5(J = 1/2)$ [3–10] and $d^1(J = 3/2)$ [11,12] compounds. Similar SOC effects can be realized also in non-Kramers d^2 oxides [13,14] with $J = 2$.

A conceptually different situation can be encountered in Mott insulators with TM ions of Van Vleck–type, i.e., when SOC imposes a nonmagnetic GS with $J = 0$ and the magnetism is entirely due to virtual transitions to higher levels with finite J. Such "nonmagnetic" Mott insulators are natural for $4d$ and $5d$ TM ions with the t_{2g}^4 configuration, e.g., Re^{3+}, Ru^{4+}, Os^{4+}, and Ir^{5+}. These ions realize a low-spin $S = 1$ state because of moderate Hund's coupling J_H (compared to $10Dq$ octahedral splitting), and, at the same time, SOC $\lambda(\boldsymbol{S} \cdot \boldsymbol{L})$ is strong enough to stabilize the $J = 0$ state gaining energy λ relative to the excited $J = 1$ triplet. Since the singlet-triplet splitting for these ions $\lambda \sim 50$–200 meV [15,16] is comparable to SE energy scales $4t^2/U \sim 50$–100 meV, we may expect magnetic condensation of Van Vleck excitons. This brings us to the "singlet-triplet" physics widely discussed in the literature in various contexts: magnon condensation in quantum dimer models [17–21], bilayer magnets [22], excitons in rare-earth filled skutterudites [23–25], a curious case of e_g orbital $FeSc_2S_4$ [26], spin-state transition in Fe pnictides [27], etc. The underlying physics and, hence, the energy scales involved in the present case are of course different from the above examples.

In this Letter, we develop a microscopic theory of the magnetism for Van Vleck-type d^4 Mott insulators. First, we derive an S and L based SE Hamiltonian and map it onto a singlet-triplet low-energy Hilbert space. We then show, taking perovskite lattices as an example, how an excitonic magnetic order, magnons, and the amplitude ("Higgs") modes do emerge in the model. Considering the model on a honeycomb lattice, we reveal the emergent one-dimensional dynamics of Van Vleck excitons and discuss possible implications of this observation.

The spin-orbital superexchange.—Kugel-Khomskii-type interactions between t_{2g}^4 ions are derived in a standard way, by integrating out oxygen-mediated d-p-d electron hoppings. We label d_{yz}, d_{zx}, and d_{xy} orbitals by a, b, and c,

respectively. In 180° (90°) d-p-d bonding geometry corresponding to corner-shared (edge-shared) octahedra, two orbitals are active on a given bond (see Fig. 2 of Ref. [5]), while the third one, say, γ, is not; accordingly, this bond is denoted by γ. Then, nearest-neighbor hoppings on the c bond read as $t(a_i^\dagger a_j + b_i^\dagger b_j + \text{H.c.})$ for 180° and $t(a_i^\dagger b_j + b_i^\dagger a_j + \text{H.c.})$ for 90° geometries. In calculations, it is helpful to introduce A, B, C operators that represent three different orbital configurations $A = \{a^2bc\}$, $B = \{ab^2c\}$, and $C = \{abc^2\}$ of the t_{2g}^4 shell and its effective $L = 1$ momentum $L_x = -i(B^\dagger C - C^\dagger B)$, etc., similar to the d^1 case [2]. [There is one-to-one correspondence $(A, B, C) \leftrightarrow (a, b, c)$ and $L^\alpha \leftrightarrow l^\alpha$ between d^4 and d^1 orbital configurations.]

The resulting spin-orbital Hamiltonian reads as $H = (t^2/U)\sum_{\langle ij\rangle}[(\boldsymbol{S_i}\cdot\boldsymbol{S_j}+1)O_{ij}^{(\gamma)} + (L_i^\gamma)^2 + (L_j^\gamma)^2]$, where $U \gg t$, λ, J_H is Hubbard repulsion. The bond-dependent orbital operator $O^{(\gamma)}$ depends on the above A, B, C; we show it directly in terms of $\boldsymbol{L}$:

$$O_{ij}^{(c)} = (L_i^x L_j^x)^2 + (L_i^y L_j^y)^2 + L_i^x L_i^y L_j^y L_j^x + L_i^y L_i^x L_j^x L_j^y. \quad (1)$$

This result holds for 180° bonding. For 90° geometry, one has simply to interchange $L_j^x \leftrightarrow L_j^y$; this can be traced back to the $a_j \leftrightarrow b_j$ relation between 180° and 90° hoppings given above. Operators $O^{(a)}$ and $O^{(b)}$ for a, b bonds follow from cyclic permutations among L_x, L_y, L_z.

The above model H operates within the $|M_S, M_L\rangle$ basis. We project it onto the low-energy subspace spanned by the GS $J = 0$ singlet $|0\rangle = \frac{1}{\sqrt{3}}(|1,-1\rangle - |0,0\rangle + |-1,1\rangle)$, and $J = 1$ triplet $|T_0\rangle = \frac{1}{\sqrt{2}}(|1,-1\rangle - |-1,1\rangle)$, $|T_{\pm1}\rangle = \pm\frac{1}{\sqrt{2}}(|\pm1,0\rangle - |0,\pm1\rangle)$ at energy $E_T = \lambda$, as dictated by local SOC. (The high-energy $J = 2$ level at 3λ is neglected.) Calculating matrix elements of S^α, L^α, and their combinations within this Hilbert space, we represent them in terms of the hard-core "triplon" $\boldsymbol{T}$ with the Cartesian components $T_x = \frac{1}{i\sqrt{2}}(T_1 - T_{-1})$, $T_y = \frac{1}{\sqrt{2}}(T_1 + T_{-1})$, $T_z = iT_0$, and "spin" $\boldsymbol{J} = -i(\boldsymbol{T}^\dagger \times \boldsymbol{T})$. For instance, $\boldsymbol{S} = -i\sqrt{\frac{2}{3}}(\boldsymbol{T} - \boldsymbol{T}^\dagger) + \frac{1}{2}\boldsymbol{J}$, $\boldsymbol{L} = i\sqrt{\frac{2}{3}}(\boldsymbol{T} - \boldsymbol{T}^\dagger) + \frac{1}{2}\boldsymbol{J}$. A projection $H(S, L) \rightarrow H(T, J)$ results in the effective singlet-triplet models $H_{\text{eff}}(180°)$ and $H_{\text{eff}}(90°)$ discussed shortly below.

In terms of $\boldsymbol{T}$ and $\boldsymbol{J}$, the magnetic moment of a t_{2g}^4 shell $\boldsymbol{M} = 2\boldsymbol{S} - \boldsymbol{L}$ reads as $\boldsymbol{M} = -i\sqrt{6}(\boldsymbol{T} - \boldsymbol{T}^\dagger) + g_J\boldsymbol{J}$ with $g_J = 1/2$, or $\boldsymbol{M} = 2\sqrt{6}\boldsymbol{v} + g_J\boldsymbol{J}$, introducing real fields $\boldsymbol{u}$ and $\boldsymbol{v}$ as $\boldsymbol{T} = \boldsymbol{u} + i\boldsymbol{v}$ with $u^2 + v^2 \le 1$ [28]. The two-component structure of $\boldsymbol{M}$ highlights a physical distinction between conventional Mott insulators, where $\boldsymbol{M}$ is simply $g_J\boldsymbol{J}$ with finite J in the GS, and the present case, where the magnetic moment resides predominantly on singlet-triplet Van Vleck transitions represented by the $\boldsymbol{T}$ exciton (hence the term "excitonic magnetism"). On the formal side, these two components obey different commutation rules, hard-core boson $\boldsymbol{T}$ vs spin $\boldsymbol{J}$; consequently, magnetic order is realized here as the Bose condensation of $\boldsymbol{T}$ particles, instead of the usual freezing of the preexisting $\boldsymbol{J}$ moments. The above equations for $\boldsymbol{S}$ and $\boldsymbol{L}$ make it also clear that $\boldsymbol{T}$ condensation implies a condensation of $\boldsymbol{S}$ and $\boldsymbol{L}$ moments resulting in finite $\boldsymbol{M}$, while the sum $\boldsymbol{S} + \boldsymbol{L} = \boldsymbol{J}$ may still fluctuate [29]. As in singlet-triplet models in general, the magnetic exciton condensation in t_{2g}^4 Van Vleck systems requires a critical exchange coupling t^2/U, so there will be a magnetic order-disorder critical point that can be tuned by pressure, doping, etc.

Singlet-triplet model $H_{\text{eff}}(180°)$.—This case applies to perovskites like ABO_3 or A_2BO_4 with corner-shared BO_6 octahedra (e.g., Ca_2RuO_4). We shape the model in the form of $H_{\text{eff}} = \lambda\sum_i n_i + (t^2/U)\sum_{\langle ij\rangle}(h_2 + h_3 + h_4)_{ij}^{(\gamma)}$, where h_2 term is quadratic in T bosons, while h_3 and h_4 represent three- and four-boson interactions, respectively [30]. For the $\gamma = c$ bond,

$$h_2^{(c)} = \frac{11}{3}\boldsymbol{v}_i\cdot\boldsymbol{v}_j - v_{iz}v_{jz} + \frac{1}{3}(\boldsymbol{u}_i\cdot\boldsymbol{u}_j - u_{iz}u_{jz}),$$
$$h_3^{(c)} = \frac{1}{\sqrt{24}}(\boldsymbol{v}_i\cdot\boldsymbol{J}_j + v_{iz}J_{jz} + u_{ix}Q_{jx} - u_{iy}Q_{jy}) + (i \leftrightarrow j),$$
$$h_4^{(c)} = \frac{3}{4}d_{ij}^\dagger d_{ij} + \frac{1}{2}\boldsymbol{J}_i\cdot\boldsymbol{J}_j + \frac{1}{4}(J_{iz}J_{jz} + J_{iz}^2J_{jz}^2) - \frac{5}{36}n_in_j. \quad (2)$$

$h^{(\gamma)}$ for $\gamma = a$, b follow from permutations among x, y, z. $n = \sum_\gamma T_\gamma^\dagger T_\gamma$, while $Q_x = -(T_y^\dagger T_z + T_z^\dagger T_y)$, etc., are quadrupole operators of T_{2g} symmetry [31]. As expected, h_4 contains a biquadratic Heisenberg coupling; we show it here via the bond-singlet operator $d_{ij} = \frac{1}{\sqrt{3}}(\boldsymbol{T}_i\cdot\boldsymbol{T}_j)$ using the identity $(\boldsymbol{J}_i\cdot\boldsymbol{J}_j)^2 = 3d_{ij}^\dagger d_{ij} + n_in_j$.

We quantify exchange interaction by $\kappa = 4t^2/U$. On a cubic (square) lattice, the model undergoes a magnetic phase transition at $\kappa_c \simeq \frac{2}{5}\lambda$ ($\kappa_c \simeq \frac{3}{5}\lambda$), due to condensation of a dipolar $\boldsymbol{v}$ part of the $\boldsymbol{T}$ bosons. The density of out-of-condensate T particles and, hence, $\boldsymbol{J}$ and Q_α are very small near critical κ, e.g., $\langle J_z^2\rangle_{\kappa_c} \sim 1/8z$ with $z = 6(4)$ for a cubic (square) lattice; thus, the interactions $h_{3,4}$ are not of a qualitative importance for the 180° case, and we focus on a quadratic part H_2 of H_{eff}. Also, bond-dependent terms in h_2 are weak and unessential in 180° geometry, so we may average them out: $v_{i\gamma}v_{j\gamma} \rightarrow \boldsymbol{v}_i\cdot\boldsymbol{v}_j/3$ for simplicity [32]. The resulting hard-core boson Hamiltonian

$$H_2 = \lambda\sum_i n_i + \kappa\frac{2}{9}\sum_{ij}[\boldsymbol{T}_i^\dagger\cdot\boldsymbol{T}_j - \frac{7}{16}(\boldsymbol{T}_i\cdot\boldsymbol{T}_j + \text{H.c.})] \quad (3)$$

is treated in a standard way familiar from "singlet-triplet model" literature (see, e.g., Refs. [17,22]).

In a paramagnetic phase $\kappa < \kappa_c$, magnetic excitations are degenerate, and their dispersion $\omega_{x/y/z}(\boldsymbol{k}) = \lambda\sqrt{1 + (\kappa/\kappa_c)\phi_{\boldsymbol{k}}}$ with $\phi_{\boldsymbol{k}} = 2/z\sum_\gamma\cos(k_\gamma)$ has a finite gap $\lambda\sqrt{1 - (\kappa/\kappa_c)}$. At $\kappa = \kappa_c$, the gap closes, and, say,

the T_z boson condenses to give a finite staggered magnetization $M_z = 2\sqrt{6\rho(1-\rho)}$ at $\kappa > \kappa_c$, where $\rho = \frac{1}{2} \times (1 - \tau^{-1})$ is the condensate density expressed via the dimensionless parameter $\tau = \kappa/\kappa_c > 1$. The M-length fluctuations, i.e., the amplitude Higgs mode, has a dispersion $\omega_z(\boldsymbol{k}) \simeq \lambda\sqrt{\tau^2 + \phi_{\boldsymbol{k}}}$ with the gap $\Delta = \lambda\sqrt{\tau^2 - 1}$, while $T_{x/y}$ excitons become gapless Goldstone magnons with the energy $\omega_{x/y}(\boldsymbol{k}) \simeq \lambda\frac{\tau+1}{2}\sqrt{1 + \phi_{\boldsymbol{k}}}$.

We are ready to show our theory in action, by applying it to the d^4 Mott insulator Ca_2RuO_4 [34] where a sizable value of the LS product has indeed been observed [35]. This fact implies the presence of an unquenched spin-orbit coupling, which is the basic input of our model.

First, we compare the observed staggered moment $M \simeq 1.3\mu_B$ [36] with our result $M = \sqrt{6(1-\tau^{-2})}\mu_B$ and find $\tau \simeq 1.18$; i.e., this compound is rather close to the magnetic critical point. For spin-orbit coupling $\lambda(= \xi/2) \simeq 75$ meV [35], this translates into $(4t^2/U) \simeq 53$ meV, a reasonable value for t_{2g} systems with $t \sim 0.2$ eV and $U \sim 3$–4 eV.

Second, using spin and orbital moments in the condensate $S = -L = \frac{1}{3\mu_B}M$, we estimate their product $LS \simeq -0.2$, which is not too far from the -0.28 ± 0.07 observed [35].

Third, we obtain from our theory the uniform magnetic susceptibility $\chi = (12\mu_B^2 N_A/\lambda(1+\tau)) \simeq 2.3 \times 10^{-3}$ emu/mol, which is consistent with that of Ca_2RuO_4 ($\sim 2.5 \times 10^{-3}$ emu/mol [34,36]) above the Néel temperature, where it is only weakly temperature dependent as expected for Van Vleck-type systems.

With the above numbers at hand (in fact, all extracted from the data), we predict the amplitude-mode gap $\Delta \sim 45$ meV and the topmost energies ~ 115 meV for all three magnetic modes. We are not aware of inelastic magnetic data for Ca_2RuO_4 to date; resonant x-ray or neutron scattering experiments would provide a crucial test for the theory.

We now turn to compounds with 90° d-p-d bonding geometry, where effective interactions lead to remarkable features not present in perovskites.

Singlet-triplet model $H_{\rm eff}(90°)$.—This case is relevant to delafossite ABO_2 or A_2BO_3 structures where BO_6 octahedra share the edges and TM ions form triangular or honeycomb lattices (e.g., Li_2RuO_3). Using the same notations as above, we find

$$
\begin{aligned}
h_2^{(c)} &= 3(\boldsymbol{v}_i \cdot \boldsymbol{v}_j - v_{iz}v_{jz}) - \frac{1}{3}(\boldsymbol{u}_i \cdot \boldsymbol{u}_j - u_{iz}u_{jz}) \\
&\equiv \frac{2}{3}(T_{ix}^\dagger T_{jx} + T_{iy}^\dagger T_{jy}) - \frac{5}{6}(T_{ix}T_{jx} + T_{iy}T_{jy}) + \text{H.c.}, \\
h_3^{(c)} &= \frac{1}{\sqrt{24}}(3\boldsymbol{v}_i \cdot \boldsymbol{J}_j + 3v_{iz}J_{jz} - u_{ix}Q_{jx} + u_{iy}Q_{jy}) + (i \leftrightarrow j), \\
h_4^{(c)} &= -\frac{3}{4}d_{ij}^\dagger d_{ij} + \frac{1}{4}(J_{iz}J_{jz} + Q_{iz}Q_{jz}) \\
&\quad + \frac{1}{6}(n_i n_{jz} + n_{iz}n_j) - \frac{1}{12}n_i n_j. \qquad (4)
\end{aligned}
$$

Again, $h^{(\gamma)}$ for $\gamma = a, b$ follow from x, y, z-cyclic permutations. While the bond-dependent nature of $h^{(\gamma)}$ is expected for SOC models on general grounds [3], it is surprising that interactions are of the same strength as in perovskites. This is in sharp contrast to $d^5(J = 1/2)$ Kramers ions, for which the leading exchange term vanishes and the form of the Hamiltonian is decided by smaller and competing effects of lattice distortions, Hund's coupling, higher-lying e_g orbital, etc. [3–5,8]. Here, no cancellation of d-p-d hoppings occurs, and magnetic coupling is of the scale of $4t^2/U$ and hence strong, which is unusual for edge-shared oxides in general. This implies robustness of the physics discussed here against distortions, etc., an important point for the material design.

We start again with the quadratic part of $H_{\rm eff}(90°)$ which reads as

$$
\begin{aligned}
H_2 = \lambda\sum_i n_i + \kappa\frac{1}{6}\sum_{ij}[(\boldsymbol{T}_i^\dagger \cdot \boldsymbol{T}_j - T_{i\gamma}^\dagger T_{j\gamma}) \\
- \frac{5}{8}(\boldsymbol{T}_i \cdot \boldsymbol{T}_j - T_{i\gamma}T_{j\gamma} + \text{H.c.})]. \qquad (5)
\end{aligned}
$$

It is clear from Eqs. (4) and (5) [see also Figs. 1(a) and 1(b)] that, on each bond, two types of bosons are only active. Consequently, a given boson flavor T_γ selects two types of bonds where it can move. For a triangular lattice, this is not crucial, though: Each flavor T_γ forms its own square-type sublattice, so the vector field $\boldsymbol{v}$ eventually condenses into a conventional 120° Néel ground state as soon as

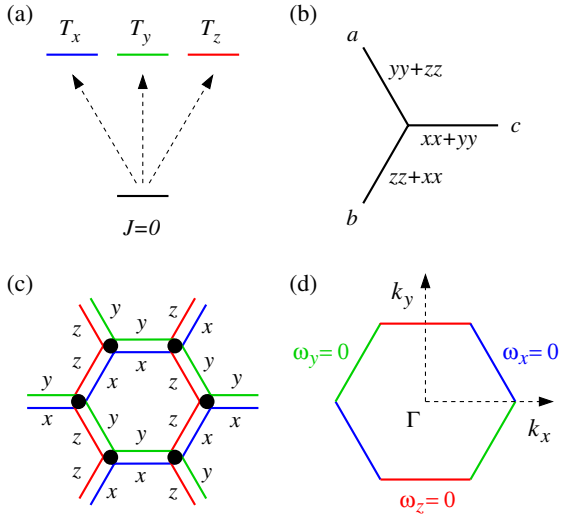

FIG. 1 (color online). Schematic of T-exciton dynamics in 90°-bonding geometry. (a) Three types of T excitations. (b) Three types of bonds on triangular or honeycomb lattices; $xx + yy$ indicates that only T_x and T_y bosons can move along c bonds. (c) On a honeycomb lattice, each type of exciton forms its own zigzag chain, e.g., z path, for T_z. (d) In momentum space, each T_γ boson softens and forms a quasicondensate at the respective edges of the Brillouin zone where $\omega_\gamma = 0$ [52].

$\kappa > \kappa_c = \frac{4}{3}\lambda$. Details can be worked out along the lines of the previous section; we focus instead on a honeycomb lattice below.

On a honeycomb (''depleted'' triangular) lattice, each boson can move along a particular zigzag chain only; see Fig. 1(c). Such a bond-and-flavor selective feature resembles that of the honeycomb Kitaev model [37], but we are dealing here with vector bosons, not spins, and this brings about interesting new physics.

In a paramagnetic phase, dispersion of the T_z boson $\omega_z(\boldsymbol{k}) \equiv \omega_z(k_y) \simeq \lambda\sqrt{1 + (\kappa/\kappa_c)c_y}$ with $c_y = \cos(\frac{\sqrt{3}}{2}k_y)$ is purely one-dimensional. As $\kappa \to \kappa_c = \frac{4}{3}\lambda$, a flat zero mode emerges at the Brillouin zone (BZ) edge $k_y = \pm\frac{2\pi}{\sqrt{3}}$. Similarly, T_x and T_y boson dispersions collapse at the other edges corresponding to x and y zigzag directions, encircling thereby the BZ by the critical $\boldsymbol{k}$ lines [Fig. 1(d)].

Thus, for $\kappa > \kappa_c$, a strongly interacting, multicolor quasicondensate emerges. The fate of this critical system is decided by $h_{3,4}$ interactions in Eq. (4) which, in contrast to the previous section, become of paramount importance. In particular, the largest amplitude, bond-singlet density term $-d_{ij}^\dagger d_{ij}$ in h_4 deserves special attention. This interaction tends to bind the $\boldsymbol{T}$ bosons into singlet pairs, cooperating thereby with a pair-generation term $\boldsymbol{T}_i \cdot \boldsymbol{T}_j \propto d_{ij}$ in Eq. (5). Put another way, its equivalent, i.e., biquadratic exchange $-(\boldsymbol{J}_i \cdot \boldsymbol{J}_j)^2$, is known to favor spin-singlet or spin-nematic states over magnetic order [38–40].

We encounter here the rich and highly nontrivial problem which requires in-depth studies using the field-theory as well as numerical methods; this goes beyond the scope of the present work. We may, however, indicate potential instabilities and possible scenarios.

The Hamiltonian (4) possesses a threefold symmetry (originating from t_{2g} orbital degeneracy): C_3 rotation of the lattice and permutation among T_x, T_y, T_z flavors. This discrete symmetry can be broken at a finite temperature. One may expect at least three distinct ground states as a function of κ: a trivial paramagnet below $\kappa_{c1} \lesssim \frac{4}{3}\lambda$; a long-range magnetic order when boson density becomes large at $\kappa_{c2} > \frac{4}{3}\lambda$; and an intermediate phase at $\kappa_{c1} < \kappa < \kappa_{c2}$ hosting the spin singlet GS. The most intriguing option for the latter is a spin-superfluid state, often discussed in the context of spin-one bosons [41] and bilinear-biquadratic spin models [42]. Here, this state is supported by a flavor-symmetric attraction $-d_{ij}^\dagger d_{ij}$ between T_γ, selecting a global spin singlet of A_{1g} symmetry where all three flavors form pairs and condense, but there is a single-particle gap. Another possibility, favored by the bond-directional nature of hoppings and interactions in Eq. (4), is a nematic order, i.e., spontaneous selection of a particular zigzag out of three x, y, z directions (assisted in real systems by electron-lattice coupling). Once a zigzag chain is formed, it can dimerize due to biquadratic interactions [38,40,43]. In other words, boson pairs condense into a valence-bond-solid pattern, followed by a suppression of Van Vleck susceptibility. Future studies are necessary to clarify the phase behavior of the model near the magnetic critical point.

In the recent past, some unusual properties of ruthenate compounds have been reported, including the formation of one-dimensional, spin-gapped chains in $Tl_2Ru_2O_7$ [44] and singlet dimers in $La_4Ru_2O_{10}$ [45,46]. Of particular interest is a honeycomb lattice La_2RuO_3 [47] which forms dimerized zigzag chains. This observation has been discussed in terms of orbital ordering [48]; the present model based on spin-orbit coupling may provide an alternative way. Indeed, a z-type zigzag chain dimerized by biquadratic exchange (and supported by electron-lattice coupling) would give the same pattern as observed [47]. Future experiments, in particular, a direct measurement of the LS product, should tell whether an unquenched L moment (the key ingredient of our model) is present in these compounds, in order to put the above ideas on more solid ground.

On the theory side, apart from low-energy properties of the model itself, important questions are related to doping of Van Vleck-type d^4 insulators. A doped electron, i.e., $J = 1/2$ fermion moving on a background of the singlet-triplet d^4 lattice, should have a large impact on magnetism and vice versa. Unconventional pairing via the exchange of T excitons also deserves attention, in particular, on triangular and honeycomb lattices (where unusual pairing symmetries have been suggested for d^5 systems with strong SOC [3,49–51]). We recall that energy scales involved in d^4 systems are large even for 90° d-p-d bonding, so all the ordering phenomena are expected at higher temperatures than in d^5 compounds like triangular lattice Na_xCoO_2 or honeycomb Na_2IrO_3.

In conclusion, unconventional magnetism emerging from exciton condensation, rather than from orientation of the preexisting local moments, can be realized in Mott insulators of Van Vleck-type ions with a nonmagnetic ground state. We derived effective models describing the magnetic condensate and its elementary excitations on various lattices. Of particular interest is the emergence of a quasi-one-dimensional condensate of magnetic excitons on a honeycomb lattice. We discussed the implications of the theory for candidate Van Vleck-type Mott insulators.

We thank J. Chaloupka, B. J. Kim, and A. Schnyder for discussions.

[1] M. Imada, A. Fujimori, and Y. Tokura, Rev. Mod. Phys. **70**, 1039 (1998).
[2] G. Khaliullin and S. Okamoto, Phys. Rev. Lett. **89**, 167201 (2002); Phys. Rev. B **68**, 205109 (2003).
[3] G. Khaliullin, Prog. Theor. Phys. Suppl. **160**, 155 (2005).
[4] G. Chen and L. Balents, Phys. Rev. B **78**, 094403 (2008).

[5] G. Jackeli and G. Khaliullin, Phys. Rev. Lett. **102**, 017205 (2009).

[6] A. Shitade, H. Katsura, J. Kuneš, X.-L. Qi, S.-C. Zhang, and N. Nagaosa, Phys. Rev. Lett. **102**, 256403 (2009).

[7] B. J. Kim, H. Ohsumi, T. Komesu, S. Sakai, T. Morita, H. Takagi, and T. Arima, Science **323**, 1329 (2009).

[8] J. Chaloupka, G. Jackeli, and G. Khaliullin, Phys. Rev. Lett. **105**, 027204 (2010); **110**, 097204 (2013).

[9] S. Bhattacharjee, S.-S. Lee, and Y. B. Kim, New J. Phys. **14**, 073015 (2012).

[10] W. Witczak-Krempa, G. Chen, Y. B. Kim, and L. Balents, arXiv:1305.2193 [Annu. Rev. Condens. Matter Phys. (to be published)].

[11] G. Jackeli and G. Khaliullin, Phys. Rev. Lett. **103**, 067205 (2009).

[12] G. Chen, R. Pereira, and L. Balents, Phys. Rev. B **82**, 174440 (2010).

[13] G.-W. Chern and N. Perkins, Phys. Rev. B **80**, 180409(R) (2009).

[14] G. Chen and L. Balents, Phys. Rev. B **84**, 094420 (2011).

[15] A. Abragam and B. Bleaney, *Electron Paramagnetic Resonance of Transition Ions* (Clarendon, Oxford, 1970).

[16] B. N. Figgis and M. A. Hitchman, *Ligand Field Theory and Its Applications* (Wiley-VCH, New York, 2000).

[17] M. Matsumoto, B. Normand, T. M. Rice, and M. Sigrist, Phys. Rev. B **69**, 054423 (2004).

[18] T. Giamarchi, Ch. Rüegg, and O. Tchernyshyov, Nat. Phys. **4**, 198 (2008).

[19] Ch. Rüegg, B. Normand, M. Matsumoto, A. Furrer, D. F. McMorrow, K. W. Krämer, H.-U. Güdel, S. N. Gvasaliya, H. Mutka, and M. Boehm, Phys. Rev. Lett. **100**, 205701 (2008).

[20] S. Sachdev and B. Keimer, Phys. Today **64**, No. 2, 29 (2011).

[21] Y. Kulik and O. P. Sushkov, Phys. Rev. B **84**, 134418 (2011).

[22] T. Sommer, M. Vojta, and K. W. Becker, Eur. Phys. J. B **23**, 329 (2001).

[23] K. Kuwahara, K. Iwasa, M. Kohgi, K. Kaneko, N. Metoki, S. Raymond, M.-A. Méasson, J. Flouquet, H. Sugawara, Y. Aoki, and H. Sato, Phys. Rev. Lett. **95**, 107003 (2005).

[24] S. Raymond, K. Kuwahara, K. Kaneko, K. Iwasa, M. Kohgi, A. Hiess, M.-A. Méasson, J. Flouquet, N. Metoki, H. Sugawara, Y. Aoki, and H. Sato, J. Phys. Soc. Jpn. **77**, 25 (2008).

[25] R. Shiina, J. Phys. Soc. Jpn. **73**, 2257 (2004).

[26] G. Chen, L. Balents, and A. P. Schnyder, Phys. Rev. Lett. **102**, 096406 (2009).

[27] J. Chaloupka and G. Khaliullin, Phys. Rev. Lett. **110**, 207205 (2013).

[28] The $(\boldsymbol{u}, \boldsymbol{v})$ representation is often more convenient, in particular, for semiclassical analysis. Physically, $\boldsymbol{v}$ takes care of a magnetic dipole carried by the $\boldsymbol{T}$ exciton (and hence enters in $\boldsymbol{S}$, $\boldsymbol{L}$, and $\boldsymbol{M}$), while $\boldsymbol{u}$ stands for the quadrupolar component of $\boldsymbol{T}$.

[29] In the $(\boldsymbol{u}, \boldsymbol{v})$ representation, $\boldsymbol{J} = 2(\boldsymbol{u} \times \boldsymbol{v})$. We will see that $\boldsymbol{v}$ condenses at the critical point but $\boldsymbol{u}$ remains fluctuating.

[30] We neglect here a small correction to singlet-triplet splitting λ arising from single-ion energy shifts; for a cubic lattice, the renormalization is $\lambda \to \lambda - (2t^2/3U)$, and even smaller for the low-coordination square and honeycomb lattices.

[31] Quadrupoles Q arise from the mapping of composite spin-orbital terms $S^\alpha L^\beta$ in H, e.g., $S^y L^z = \sqrt{\frac{2}{3}} u_x + \frac{1}{2} Q_x$. Note that $\boldsymbol{u}$ enters here, revealing its quadrupole nature.

[32] The only effect of small "compasslike" $v_{i\gamma} v_{j\gamma}$ terms here is to select an easy magnetic axis and open (order-by-disorder) magnon gap that can be routinely worked out [33].

[33] G. Khaliullin, Phys. Rev. B **64**, 212405 (2001).

[34] S. Nakatsuji, S. Ikeda, and Y. Maeno, J. Phys. Soc. Jpn. **66**, 1868 (1997).

[35] T. Mizokawa, L. H. Tjeng, G. A. Sawatzky, G. Ghiringhelli, O. Tjernberg, N. B. Brookes, H. Fukazawa, S. Nakatsuji, and Y. Maeno, Phys. Rev. Lett. **87**, 077202 (2001).

[36] M. Braden, G. André, S. Nakatsuji, and Y. Maeno, Phys. Rev. B **58**, 847 (1998).

[37] A. Kitaev, Ann. Phys. (Amsterdam) **321**, 2 (2006).

[38] A. V. Chubukov, Phys. Rev. B **43**, 3337 (1991).

[39] E. Demler and F. Zhou, Phys. Rev. Lett. **88**, 163001 (2002); A. Imambekov, M. Lukin, and E. Demler, Phys. Rev. A **68**, 063602 (2003).

[40] S. K. Yip, Phys. Rev. Lett. **90**, 250402 (2003).

[41] F. H. L. Essler, G. V. Shlyapnikov, and A. M. Tsvelik, J. Stat. Mech. (2009) P02027.

[42] M. Serbyn, T. Senthil, and P. A. Lee, Phys. Rev. B **84**, 180403(R) (2011).

[43] Z.-X. Liu, Y. Zhou, H.-H. Tu, X.-G. Wen, and T.-K. Ng, Phys. Rev. B **85**, 195144 (2012).

[44] S. Lee, J.-G. Park, D. T. Adroja, D. Khomskii, S. Streltsov, K. A. McEwen, H. Sakai, K. Yoshimura, V. I. Anisimov, D. Mori, R. Kanno, and R. Ibberson, Nat. Mater. **5**, 471 (2006).

[45] P. Khalifah, R. Osborn, Q. Huang, H. W. Zandbergen, R. Jin, Y. Liu, D. Mandrus, and R. J. Cava, Science **297**, 2237 (2002).

[46] Hua Wu, Z. Hu, T. Burnus, J. D. Denlinger, P. G. Khalifah, D. G. Mandrus, L.-Y. Jang, H. H. Hsieh, A. Tanaka, K. S. Liang, J. W. Allen, R. J. Cava, D. I. Khomskii, and L. H. Tjeng, Phys. Rev. Lett. **96**, 256402 (2006).

[47] Y. Miura, Y. Yasui, M. Sato, N. Igawa, and K. Kakurai, J. Phys. Soc. Jpn. **76**, 033705 (2007).

[48] G. Jackeli and D. I. Khomskii, Phys. Rev. Lett. **100**, 147203 (2008).

[49] G. Khaliullin, W. Koshibae, and S. Maekawa, Phys. Rev. Lett. **93**, 176401 (2004).

[50] T. Hyart, A. R. Wright, G. Khaliullin, and B. Rosenow, Phys. Rev. B **85**, 140510(R) (2012).

[51] Y-Z. You, I. Kimchi, and A. Vishwanath, Phys. Rev. B **86**, 085145 (2012).

[52] We may reverse the sign of κ in Eq. (5) by virtue of the four-sublattice transformation [3]. Then, zero-energy lines would go through the Γ point, e.g., $\omega_z(\boldsymbol{k}) = 0$ at $k_y = 0$.